Top Med Chem (2019) 32: 133–156
DOI: 10.1007/7355_2018_50

Published online: 27 August 2019

HCV NS5A as an Antiviral Therapeutic Target: From Validation to the Discovery and Development of Ombitasvir and Pibrentasvir as Components of IFN-Sparing HCV Curative Treatments

Rolf Wagner, David A. DeGoey, John T. Randolph, Allan C. Krueger, Mark A. Matulenko, and Warren M. Kati

Contents

Abstract While IFN-based hepatitis C virus (HCV) treatment regimens required long treatment duration, they only achieved a limited cure rate in HCV-infected patients and were accompanied by significant therapy-based side effects. The first curative IFN-sparing therapies revolutionized HCV treatment by utilizing a cocktail of mechanistically orthogonal direct-acting antiviral (DAA) agents to achieve much higher cure rates in a shorter period of time and with fewer side effects. One of the drug targets that these therapies usually engaged was the HCV NS5A protein. This chapter reviews the Abbott/AbbVie HCV NS5A program, which discovered

R. Wagner (✉), D. A. DeGoey, J. T. Randolph, A. C. Krueger, M. A. Matulenko, and W. M. Kati
AbbVie Inc., North Chicago, IL, USA
e-mail: Rolf.Wagner@abbvie.com; David.Degoey@abbvie.com; John.Randolph@abbvie.com; A.Chris.Krueger@abbvie.com; Mark.Matulenko@abbvie.com; Warren.Kati@abbvie.com

inhibitors of this protein using an in vitro phenotypic screen, validated the mechanism in vivo, and ultimately discovered two FDA-approved NS5A inhibitors ombitasvir (OMB) and pibrentasvir (PIB). OMB, a first-generation NS5A inhibitor, is a component of two FDA-approved IFN-sparing DAA therapies (Viekira Pak™ and Technivie™) with approval to treat genotypes 1 and 4, respectively. PIB, a next-generation NS5A inhibitor included in AbbVie's next-generation therapy Mavyret™ (or Maviret™), prevents replication of HCV genotypes 1–6 and exhibits an improved resistance profile relative to other FDA-approved first-generation NS5A inhibitors.

Keywords Abbott, AbbVie, ABT-267, ABT-530, DAA, HCV, Hepatitis C, IFN-sparing, Maviret, Mavyret, NS5A, Ombitasvir, Pibrentasvir, Technivie, Viekira Pak

1 Introduction

Abbott Laboratories was one of the first companies to commercialize a blood screening test for hepatitis C virus (HCV) in 1990 and has maintained a continuous flow of improvements and new platform technologies through the present day. This early and sustained commitment to HCV by our colleagues in Abbott's Diagnostic Division, combined with the growing awareness of the significant medical need for well-tolerated and effective treatments for HCV infections, piqued the interest of the antiviral drug discovery team within the Pharmaceutical Products Division. (Note: The Pharmaceutical Products Division was spun off from Abbott as a separate company in 2013 and is now known as AbbVie). Although the antiviral drug discovery team was heavily involved in HIV research in the 1990s, work that would lead to the discovery of the marketed HIV protease inhibitors ritonavir and lopinavir, a small exploratory effort was initiated in the HCV space. Several biochemical screens were conducted to identify inhibitors of the NS3/4A protease and the NS5B RNA-dependent RNA polymerase. Whereas the protease inhibitor screen yielded very little that was ultimately useful, among the polymerase inhibitor screening hits was a fragment with weak binding affinity [1]. Elaboration of this fragment resulted in the discovery of dasabuvir, a nonnucleoside RNA polymerase inhibitor that is a component of the marketed drug for HCV genotype 1 infections known as Viekira Pak™ [2]. Beyond biochemical screens, the availability of subgenomic HCV replicons afforded the opportunity to conduct a cell-based phenotypic screen to identify inhibitors of HCV replication. The following sections in this chapter provide some detail with regard to how a compound identified in the replicon inhibition screen ultimately gave rise to ombitasvir and pibrentasvir, NS5A inhibitors that are components of the marketed HCV drug treatments Viekira Pak™ and Mavyret™, respectively.

2 Discovery of AbbVie's First-Generation HCV NS5A Inhibitors

2.1 Screening Hit and the Establishment of NS5A Inhibitors as a Viable HCV Drug Discovery Approach

A phenotypic screen was initiated in our laboratories to identify compounds that inhibited replication of the HCV genotype 1b subgenomic replicon. Naphthyridine **1** (see Fig. 1) emerged as an interesting hit from this screen, inhibiting replication of

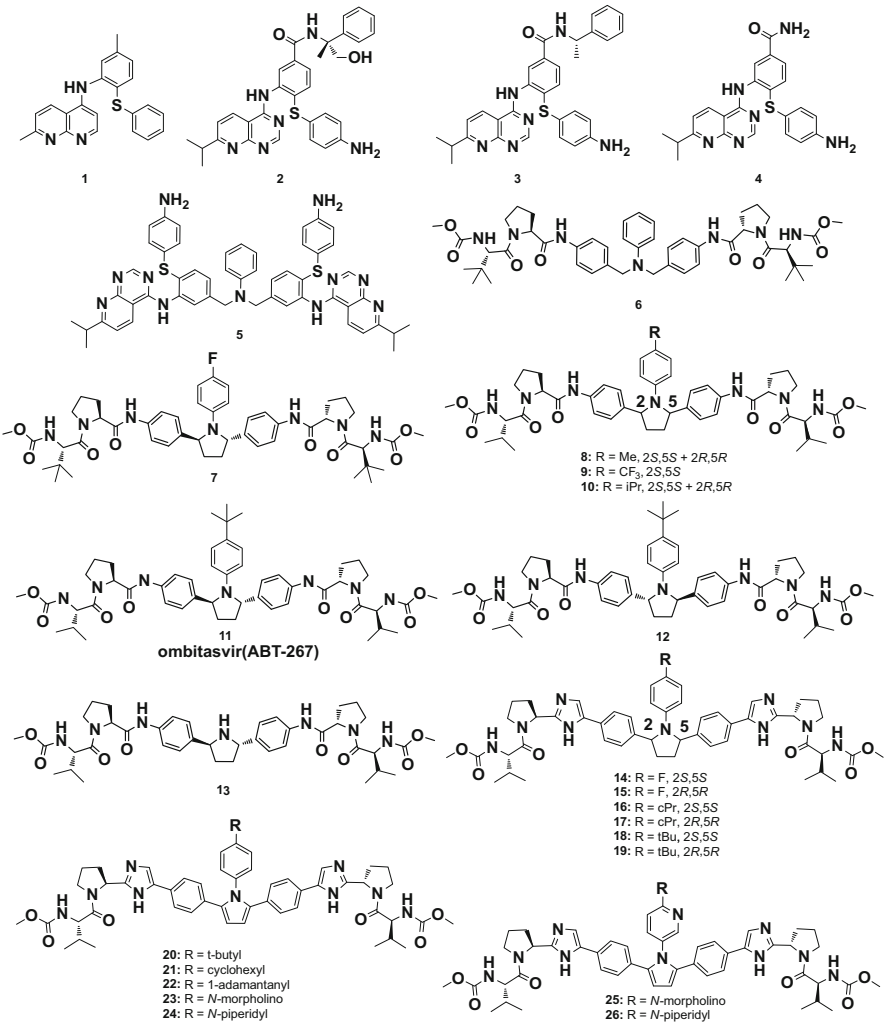

Fig. 1 Structures of NS5A inhibitors

the genotype 1b replicon with an $EC_{50} = 20$ nM, whereas cellular toxicity only occurred at concentrations that were >400-fold higher. The mechanism of action for **1** was initially elusive as it showed no inhibition in HCV NS3 protease, NS3 helicase, NS5B polymerase, HCV IRES, or EMCV IRES assays. However, treating genotype 1b replicon cells with **1** under conditions where replication of the HCV subgenome is essential for cell viability led to the selection of subgenomic variants with mutations in the NS5A gene, corresponding to amino acid substitutions at position 31 (L31F or V) or 93 (Y93C or H). Replicon cells containing the NS5A L31V or Y93C variants conferred 45–150-fold resistance toward **1**, whereas no resistance was conferred upon HCV protease or polymerase inhibitors, strongly suggesting that the mechanism of action for **1** was mediated, in some way, through the NS5A protein. Additional in vitro studies showed that the combination of **1** with HCV polymerase inhibitors could inhibit HCV subgenomic 1b replication much more effectively than when either compound was used alone, establishing **1** and its putative NS5A mechanism of action as a new class of HCV inhibitors that are synergistic when combined with the more mainstream polymerase (or protease) inhibitors.

Although these in vitro results were compelling, there was considerable uncertainty with regard to whether they would translate into robust antiviral efficacy in the in vivo setting. This uncertainty arose from the presence of adaptive mutations in the NS5A gene of the subgenomic replicon that are not present in fully genomic, infectious virus, thereby raising the possibility that the replicon inhibitory effects by NS5A inhibitors such as **1** might be an artifact of the subgenomic replicon system. Therefore, an in vivo proof-of-concept study in the HCV genotype 1b infected chimpanzee model was conducted in collaboration with the Southwest Foundation for Biomedical Research. Pyrido-pyrimidine compound **2**, with a genotype 1b replicon $EC_{50} = 80$ nM measured in the presence of 40% human plasma, elicited a 1.65 $\log_{10}$ decline in viral load in this model when IV dosed at 2.5 mg/kg q8h × 5 [6]. This clear viral load decline, coupled with the in vivo selection of NS5A L28M and Y93H resistant variants (which were also selected in in vitro experiments), validated this chemical series and replicon NS5A inhibitors in general, as a viable approach for achieving viral load declines in the in vivo setting.

2.2 *Identification of the E-Ring Pharmacophore and the Move to C-2 Symmetrical Compounds*

One of the challenges for the program was achieving potent inhibition in genotype 1a replicons. A breakthrough occurred with compound **3** which demonstrated inhibition of genotype 1a and 1b replicons with EC_{50} values in the 20–45 nM range. Notably, the close analog **4** exhibited no activity in the genotype 1a replicon at 50 μM, suggesting that the benzylic "E-ring" contributed at least 1,000-fold toward the activity of **3** in the genotype 1a replicon. Given that uniform activity in

genotypes 1a and 1b was a goal for the program, this important E-ring pharmacophore was retained throughout the duration of the project.

In a quest for identifying strategies that might lead to further potency improvements, the team was aware of the published X-ray crystal structure for the domain I form of HCV NS5A which established that this part of the HCV NS5A protein exists as a C-2 symmetrical dimer [3]. Exploiting this C-2 symmetry in some way had appeal to the team, based on its previous success in creating C-2 symmetrical inhibitors of HIV protease, likewise a C-2 symmetrical protein dimer [4]. This background, combined with emerging reports that others were having success in deriving highly potent NS5A inhibitors using a C-2 symmetric strategy stimulated an exploratory effort to create C-2 symmetrical dimeric molecules from our pyrido-pyrimidine series [5]. Compound **5** is an example from this series whose EC_{50} values of 4.9 and 0.05 nM in the genotype 1a and 1b replicons, respectively, represented at least a 9–400-fold improvement over the "monomeric" pyrido-pyrimidines such as **3** and **4**, thereby validating the C-2 symmetric approach for improving potency.

2.3 N-*Phenylpyrrolidine Series Discovery*

However, drug discovery challenges remained for the C-2 symmetric pyrido-pyrimidine series, especially with regard to achieving microsomal stability, oral bioavailability, and uniform genotype 1a/1b potency. Several strategies were investigated to address these concerns, but the most successful one involved keeping the central core with the E-ring and incorporating more drug-like ends. Compound **6** exhibited replicon potencies (EC_{50} = 7.2 and 0.1 nM toward genotype 1a and 1b replicons, respectively; see Table 1) that were comparable to **5** but had the added benefit of being at least 28% orally bioavailable as evaluated in an 8-h rat pharmacokinetic study. Attempts to improve potency and microsomal stability via conformational constraint resulted in the discovery of the *N*-phenylpyrrolidine series. 2,5-disubstituted *N*-phenyl pyrrolidine inhibitor **7** is an early compound from this series and demonstrated 23% oral bioavailability and an IV half-life in rat that was too long to be accurately measured in a 24 h pharmacokinetics study (Table 2). Compound **7** also exhibited replicon EC_{50} values that were 16–27-fold more potent than the acyclic comparator **6**. The large potency improvement for the pyrrolidine inhibitor is likely due to stabilization of an active conformation provided by the rigid heterocyclic core. The team was sufficiently encouraged by the long plasma half-life and sub-nanomolar replicon potencies to mount an extensive SAR campaign on the *N*-phenylpyrrolidine series.

Table 1 In vitro activity against HCV GT1a and GT1b in the replicon assay and ADME data

	Replicon potency (nM)[a]				ADME		
	0% human plasma		40% human plasma		Solubility[b]	% Remaining[c]	
Compd	GT1a	GT1b	GT1a	GT1b	pH 7.2	HLM	RLM
6	7.2	0.100	69	0.685	2.6	29	57
7	0.263	0.006	15.5	0.528	4.4	52	56
8	0.720	0.040	4.36	0.204	9.9	42	44
9	0.057	0.007	0.650	0.072	3.4	58	68
10	0.033	0.008	0.706	0.086	1.9	65	67
11	0.014	0.005	0.186	0.056	2.7	60	73
12	0.138	0.088	0.986	0.090	1.8	n/a[d]	65
14	0.009	0.008	0.358	0.255	1.1	37	45
15	0.029	0.009	0.714	0.297	1.2	49	48
16	0.012	0.007	0.310	0.130	4.0	36	63
17	0.005	0.008	0.094	0.094	1.3	34	68
18	0.004	0.003	0.129	0.082	1.4	73	68
19	0.003	0.004	0.061	0.078	2.9	77	70
20	0.018	0.013	0.504	0.562	<0.7	67	79
21	0.018	0.010	0.284	0.148	1.4	66	75
22	0.011	0.007	0.293	0.251	10.5	93	100
23	0.045	0.010	0.667	0.290	1.1	54	65
24	<0.1	0.010	0.249	0.159	3.7	48	82
25	0.047	0.020	0.876	0.526	2.0	29	41
26	0.008	0.008	0.178	0.144	1.6	53	61

[a]GT1a-H77 and GT1b-Con1 replicon inhibitory effects were determined as described previously
[b]Kinetic solubility (μM) determined by chemiluminescent nitrogen detection (CLND) in 10 mM phosphate buffer (pH 7.2)
[c]Percentage of parent compound remaining after 30-min incubation
[d]Not available

2.4 Phenyl-Amino Pyrrolidine Series

The objective for the team was to identify a compound for clinical development that possessed sub-nanomolar potency in both genotype 1a and 1b replicon assays, as well as cross-species pharmacokinetics that would be consistent with once-daily dosing in humans. Replicon activity was determined with and without the addition of 40% human plasma in order to assess the effect that binding to plasma proteins could have on potency of the inhibitors, in vivo. Further potency improvement was obtained with alkyl substituents in the para-position of the *N*-phenyl group, such that increasing the size of the 4-alkyl substituent provided better replicon activity, particularly in genotype 1a. Thus, 4-methyl-substituted analog **8** was 12-fold less active than 4-trifluoromethyl analog **9** and 20-fold less active than 4-isopropyl analog **10** in the 1a replicon assay (Table 1). Potency differences were more modest in the 1b replicon. Importantly, both **9** and **10** provided sub-nanomolar activity against both 1a and 1b replicons in the presence of 40% human plasma.

Table 2 Pharmacokinetic parameters for selected compounds[a]

Compd	Species	IV[b]			Oral[b]				
		$t_{1/2}$	Vss	Cl	$t_{1/2}$	T_{max}	C_{max}	AUC	F
7	Rat	NC[c]	NC[c]	<0.39	NC[c]	3.0	0.11	1.85	23
9	Rat	6.0	8.9	1.2	12.1	2.2	0.03	0.50	16
	Dog	6.0	1.3	0.16	5.8	4.7	0.07	0.85	5.5
11	Rat	9.9	5.9	0.65	15.9	3.7	0.01	0.29	6.2
	Mouse	11.0	1.7	0.11	11.1	6.0	0.38	7.65	29
	Dog	7.9	1.8	0.18	7.3	3.3	0.64	8.00	57
	Monkey	4.4	1.5	0.38	5.0	3.3	0.29	2.40	35
12	Rat	5.5	2.2	0.43	8.6	4.7	0.02	0.22	3.1
14	Rat	4.2	3.2	0.72	6.7	2.0	0.04	0.43	9.5
15	Rat	3.6	1.2	0.25	3.9	2.2	0.19	1.52	12
16[d]	Rat	5.8	3.4	0.54	7.3	3.7	0.09	1.20	19
18	Rat	6.6	2.3	0.33	11.6	2.0	0.03	0.36	3.7
19	Rat	6.1	1.5	0.34	7.2	1.5	0.02	0.17	2.0
	Mouse	NC[c]	NC[c]	0.09	NC[c]	10.0	0.14	2.23	3.9
	Dog	8.8	0.9	0.07	8.9	3.3	0.32	4.32	12
	Monkey	6.2	1.2	0.16	7.6	4.3	0.26	3.35	20
20	Rat	6.0	2.3	0.41	7.8	2.8	0.07	0.82	11
21	Rat	6.9	1.9	0.32	5.9	4.5	0.02	0.30	3.2
22	Rat	12.7	1.7	0.10	4.3	3.5	0.05	0.43	1.5
23	Rat	3.5	2.4	0.57	6.9	7.0	0.08	1.06	20
26	Rat	4.2	1.2	0.27	3.9	10.0	0.29	3.85	35
	Mouse	NC[d]	NC[d]	<0.025	NC[d]	11.0	0.85	14.4	13
	Dog	5.0	0.7	0.11	3.7	3.3	1.08	13.2	57
	Monkey	2.7	0.8	0.24	2.7	4.0	0.14	0.81	8.0

[a]Units: $t_{1/2}$ (h); Cl (L/h/kg); C_{max} (μg/mL); $AUC_{0-24\ h}$ (μg h/mL); F (%)
[b]Doses: 3 mg/kg IV and oral for rat and mouse, 1 mg/kg IV and 2.5 mg/kg oral for dog and monkey
[c]*NC* not calculated
[d]Dosed as a mixture of A-1246114.0 and A-1246108.0

The 4-tert-butylphenyl analog **11** provided 1a and 1b replicon EC_{50} values of 0.014 nM and 0.005 nM, respectively. The 40% human plasma attenuating effect on potency was just over tenfold for both genotypes. The threefold 1a/1b potency difference for **11** is in stark contrast to the >72-fold difference seen with **6**, which clearly illustrates the benefit of the pyrrolidine core for this inhibitor series. The pyrrolidine stereochemistry in **11** is important to potency, as this 2*S*,5*S*-trans isomer is tenfold more active in the 1a replicon assay when compared to the 2*R*,5*R*-trans isomer **12**. The activity difference in the 1b replicon assay was on the order of twofold, once again favoring the *S*,*S*-trans isomer **11**. While proper orientation of the substituents at positions 2 and 5 on the pyrrolidine ring is important for inhibitory effect as evidenced by the activity differences for **11** and **12**, the *t*-butylphenyl substituent on the pyrrolidine nitrogen plays an equally critical role for potency of these inhibitors. An analog that lacks this substituent (**13**) was 10,000-fold less

active than **11** in the 1a replicon assay ($EC_{50} = 2$ μM in both 1a and 1b replicon in the presence of 40% human plasma).

Pharmacokinetic profiling of promising compound **11** was conducted across species (Table 2). The pharmacokinetic profile in rat, monkey, and dog was characterized by low plasma clearance values in rat (0.46 L/h kg) and monkey (0.38 L/h kg), with even lower values in dog (0.18 L/h kg) and mouse (0.11 L/h kg). The compound was characterized by moderate to high volumes of distribution in all species (Vss), with values of 1.5–1.8 L/kg for mouse, dog, and monkey but higher values for rat (4.8 L/kg). The apparent elimination half-life ranged from 4.4 h in monkey to 11.4 h in rat. Oral bioavailability values ranged from 24.8% in rat to 57.3% in dog. The bioavailability in dog for this sparingly soluble compound was markedly affected by formulation, with slow absorption (T_{max} 12.6 h) and low bioavailability (10%) obtained from an aqueous suspension; more rapid absorption was noted with a lipid-based solution formulation (T_{max} 1.8 h), with a fourfold increase in bioavailability (*F* 41%). Compound **11** concentrations in the liver exceeded levels in the plasma by 10–12-fold at the 24-h timepoint in mice administered single doses at 1, 3, 10, or 30 mpk.

2.5 *Phenyl Imidazole Pyrrolidine Series*

In an effort to explore the effect of changes to the bis-phenyl amide linker groups in analogs such as **11**, we made some chemical modifications. One of the changes investigated was replacement of the bis-phenyl amide units with slightly longer and more acidic bis-phenyl imidazole linker units. Six of these analogs are shown in Fig. 1 (**14**–**19**). Within this set, compounds with different stereochemical configurations around the central pyrrolidine core (2*S*,5*S* and 2*R*,5*R*) in conjunction with three different "E-ring" para-phenyl substituents (fluoro, cyclopropyl, and tert-butyl) are represented. In general, the stereochemistry around the pyrrolidine core (2*S*,5*S* or 2*R*,5*R*) did not lead to significant replicon potency differences in the matched analogs (**14** and **15**, **16** and **17**, **18** and **19**). The most potent bis-phenyl imidazole analog made was **19**, which displays GT1a replicon potency in 40% human plasma of 0.061 nM and the corresponding GT1b replicon potency of 0.078 nM (Table 1). This analog displays roughly threefold better potency in GT1a and nearly equivalent GT1b potency when compared to the best bis-phenyl amide analog, **11**. It should also be noted that these two analogs surprisingly differ in their stereochemistry around the central pyrrolidine ring (2*R*,5*R* for **19** and 2*S*,5*S* for **11**). Analog **19** had similar solubility and ADME parameters when compared with **11**. The pharmacokinetic parameters of some of the bis-phenyl imidazole analogs are shown in Table 2. In general, the bis-phenyl imidazole series compounds showed lower oral bioavailability than the bis-phenyl amide analogs, with the most potent analog **19** displaying a good IV half-life and clearance in rat but with low plasma AUC and bioavailability values upon oral administration. Clearance in mouse and dog were also low with long half-life in mouse that could not be calculated from a 24 h study,

although oral bioavailability was also low in these species. In monkey, **19** also demonstrated a long IV plasma half-life with low clearance; however, the oral AUC and bioavailability values were found to be higher than in the other species.

2.6 Phenyl Imidazole Pyrrole Series

While the introduction of the pyrrolidine group resulted in improved potency and pharmacokinetics compared to the acyclic analogs, additional SAR was conducted with the goal of improving potency and PK. One approach was to design new cores that might be more synthetically accessible than the pyrrolidine core to enable more diverse E-ring SAR exploration. One such modification was to replace the pyrrolidine ring with a pyrrole, a transformation which removed two stereocenters. Initially, the pyrrole equivalent to **11** was synthesized (not pictured) and found to be about 100–300-fold less potent in both genotypes 1a and 1b. While several additional modifications to the E-ring and substitution on the pyrrole ring were attempted, we were unable to break into the sub-nanomolar potencies enjoyed by the pyrrolidine series. Incorporating the pyrrole core with the bis-phenyl imidazole series generated **20** (Fig. 1). Biochemical evaluation of this molecule found it to be the first in the pyrrole series to possess sub-nanomolar potency in the presence of 40% HP (1a/1b; 0.50 nM/0.56 nM). In rat PK studies, it demonstrated oral bioavailability comparable to **11** (see Tables 1 and 2).

Further SAR on the E-ring pocket of the pyrrole series demonstrated that similarly sized and larger substituents were tolerated without significant decreases in potency, such as cyclohexyl (**21**), adamantyl (**22**), morpholino (**23**), and piperidinyl (**24**). We found that while there was no significant change in potency, in most cases oral bioavailability was negatively impacted. One exception was *N*-morpholino compound **23** which demonstrated 20% oral bioavailability in rat. Previous experience on earlier, internal projects had shown that 2-aminopyridines sometimes had positive effects in rat oral bioavailability [7]. Thus, we synthesized and evaluated the 2-aminopyridine analogs, **25** and **26**. The more potent piperidinyl analog (**26**) showed comparable GT1a potency to **11** and improved oral bioavailability in rat PK ($F = 35\%$). The compound demonstrated a long half-life and low clearance in mouse. In dog, the compound demonstrated low clearance and high oral bioavailability (57%), although it demonstrated a short half-life and lower oral bioavailability in monkey.

2.7 Advanced Characterization and Selection of Ombitasvir (ABT-267)

Several compounds were selected for advanced characterization for potential selection as a clinical candidate. From a virological perspective, high potency against

HCV GT1a and GT1b was viewed as a necessary requirement. Based on their high potencies against GT1a and GT1b in the presence of 40% HP, **11**, **19**, and **26** underwent additional characterization. As shown in Table 3, potencies across the other genotypes were also evaluated where compound **11** showed a potential advantage over the other two compounds. Compound **11** demonstrated relatively uniform potency across the genotypes 1 through 5, with lower potency observed at GT6a. This is in contrast to compound **19** which showed lower potency at GT2a and GT3a and compound **26** which showed lower potency at GT2a, GT2b, GT3a, GT5a, and GT6a. Activity against commonly selected GT1-resistant variants in the replicon assay against NS5A inhibitors is shown in Table 4. In general, high levels of resistance were observed for several variants for all three compounds. HCV GT1a variants at M28, Q30, and Y93 conferred high resistance against compound **11**. Overall, these same variants conferred a lower level of resistance against compound **19** when compared with analog **11**. Phenyl imidazole pyrrole analog **26** demonstrated a comparable profile to **11**, although the HCV GT1b Y93H variant demonstrated higher resistance against **26** relative to **11**.

Compounds **11**, **19**, and **26** exhibited good in vitro microsomal stabilities in human and rat liver microsomes (Table 1), and metabolic stability in hepatocytes suggests low clearance across species (data not shown). The compounds showed low solubility in their amorphous forms at pH 7.2 (Table 1), while higher solubility was observed in fed and fasted simulated intestinal fluids (FeSSIF and FaSSIF). No inhibition of CYP1A2, 2C9, 2C19, 2D6, and 3A4 (IC50 $>$ 30 μM) and no significant CYP3A4 or CYP1A2 mRNA induction in human hepatocytes was observed with

Table 3 Potency across genotypes in the stable replicon assay

	Replicon EC_{50} pM (fold)[a]						
Compd	GT1a	GT2a	GT2b	GT3a	GT4a	GT5a	GT6a
11	14	12 (0.9)	4.3 (0.3)	19 (1.4)	1.7 (0.1)	3.2 (0.2)	366 (30)
19	3	159 (53)	21 (7)	578 (192)	1.9 (0.6)	n.t.[b]	n.t.[b]
26	8	62 (7.7)	1,033 (129)	4,818 (602)	3.6 (0.4)	1,820 (228)	1,536 (192)

[a]Fold loss in activity is relative to GT1a-H77
[b]*n.t.* not tested

Table 4 HCV Genotype 1a transient replicon EC_{50}s (fold resistance) for variants selected against GT1a and GT1b in vitro

	GT1a EC_{50} nM (fold)[a]						GT1b EC_{50} nM (fold)[a]	
Compd	WT	M28T	M28V	Q30R	Y93C	Y93H	WT	Y93H
11	0.0027	24.5 (9,065)	0.159 (58)	2.18 (800)	4.6 (1,675)	113 (41,383)	0.0008	0.06 (77)
19	0.0004	0.063 (146)	0.003 (6)	0.026 (61)	0.044 (102)	0.322 (742)	0.001	0.015 (15)
26	0.0023	0.473 (208)	0.006 (3)	1.27 (559)	0.674 (297)	5.8 (2,555)	0.002	1.07 (535)

[a]Fold loss in activity relative to wt

any of the three advanced analogs. Human, rat, dog, and monkey plasma protein binding was determined to be high (>99%). Observed PAMPA permeability was low for the compounds, while results from the Caco-2 model suggested that **26** has low-to-moderate permeability and were unclear for **11** and **19** due to low recovery and non-specific binding. While **11** and **19** were generally stable compounds, **26** was unstable to UV light (320–395 nm) in pH 7.4 solution. Although this sensitivity could be circumvented by proper light protection, radiolabeled tissue distribution studies in rats indicated that **26** distributed to skin (pigmented/nonpigmented) and eyes and that photo-safety testing should be conducted.

Compounds **11**, **19**, and **26** were well tolerated at the maximum oral exposures in 14-day mouse toxicology studies. In addition, they were predicted to have human half-lives consistent with QD dosing (≥12 h). Ultimately, **11** was selected as the first clinical candidate, being renamed as ABT-267, and ombitasvir in later clinical testing [8, 9]. The pharmacokinetics, safety, and tolerability were evaluated in a phase I study in healthy volunteers following single doses of 5–350 mg and multiple doses of 5–200 mg, where the half-life ranged from 18 to 26 h and 25 to 34 h, respectively [10, 11]. ABT-267 was safe and well tolerated across all dose groups. The antiviral activity of ABT-267 was initially evaluated during 3-day monotherapy in HCV GT1-infected treatment-naïve subjects at doses ranging from 5 to 200 mg [12]. On day 3, dose-normalized Cmax and AUC values were similar across doses. ABT-267 demonstrated C_{max} values ranging from 5.7 to 442 ng/mL and a half-life ranging from 25 to 32 h across the dose groups. As shown in Fig. 2, ABT-267 decreased HCV RNA up to 3.10 $\log_{10}$ IU/mL during 3-day monotherapy with a nearly 3 log reduction observed in all dose groups. The drug candidate was generally

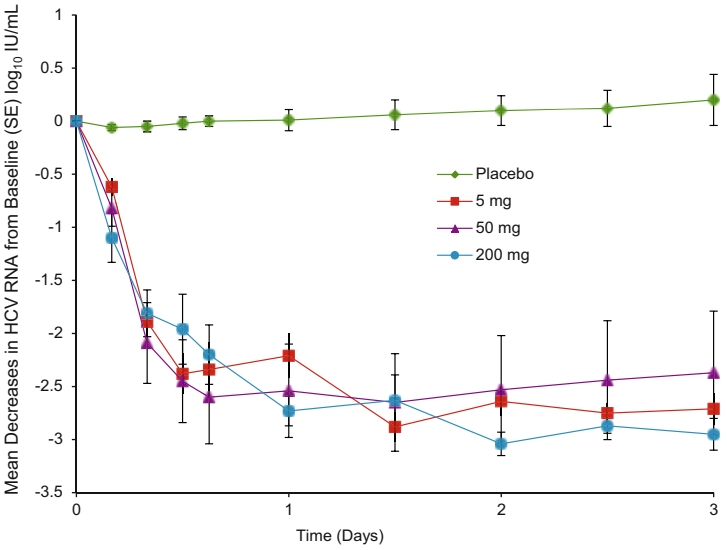

Fig. 2 Mean decreases in HCV RNA from baseline during 3-day monotherapy with ABT-267 (ombitasvir) in HCV GT1-infected treatment-naïve subjects

well tolerated at all doses, and there were no serious or severe adverse events, no clinically significant laboratory abnormalities, and no subjects discontinued. Most adverse events were mild and were not dose related. These findings supported continued development of ABT-267 as a once-daily NS5A inhibitor, and subsequent clinical trials were conducted in combination with NS5B polymerase inhibitor dasabuvir and NS3/4A protease inhibitor paritaprevir/ritonavir with or without ribavirin. Efficacy and safety data from phase III clinical trials supported the regulatory filing and marketing approval of ombitasvir (ABT-267), as part of Viekira Pak™ for the treatment of GT1 HCV in December of 2014.

3 Discovery of a Next-Generation NS5A Inhibitor [13]

While the medicinal chemistry strategy for the discovery of a next-generation NS5A inhibitor was to retain the potent antiviral properties of ombitasvir, additional improvements to genotype coverage and the resistance profile were mandatory. Furthermore, development of a compound with an improved resistance profile could potentially translate into requiring fewer DAAs in the curative combination, as well as possibly shorten the 12-week treatment duration, which, with very limited exceptions, was the most common treatment time course in first-generation peg-IFN/RBV-sparing DAA-based therapies. As shown above, AbbVie's first-generation NS5A inhibitor, ombitasvir, exhibited potent EC_{50}s (ranging 0.82–19.3 pM) against HCV genotypes 1–5 and an EC_{50} of 366 pM against genotype 6a in the replicon assays. In vitro resistance selection experiments in genotype 1–6 replicons selected variants which demonstrated reduced susceptibility to the actions of ombitasvir, by factors often greater than 1,000-fold [8]. Variants of NS5A amino acid positions 28, 30, and 93 were most commonly detected in patients experiencing virologic failure with the first-generation NS5A inhibitors ombitasvir, daclatasvir, and ledipasvir. We therefore examined the resistance profiles of the newly synthesized compounds against representative amino acid substitutions, M28T, Q30E, Q30R, Y93C, Y93H, and Y93N in genotype 1a and Y93H and Y93N in genotype 1b replicons.

An alternative inhibitor scaffold (Fig. 3 and Table 5) investigated the impact of the "linker" moiety, as well as the absolute stereochemistry at carbons 2 and 5. While the phenyl amide linker pair, present in ombitasvir and **12** (see Fig. 1), presented the desired broad genotype coverage with the chirality at carbons 2 and 5 being *S*,*S* (vide supra), the 2*S*,5*S*-benzimidazole analog **27** was weakened in genotype 1a in the presence of 40% human plasma, despite being an isosteric replacement for the linker found in ombitasvir (see Fig. 3). Surprisingly, the 2*R*,5*R* isomer (**28**) provided reasonably potent activity against most of the genotypes tested. Coupled with the reduced potency fold loss of first-generation resistant variants relative to WT genotypes 1a and 1b (see Table 7), when compared to ombitasvir, the properties of **28** indicated that this compound could serve as a promising lead for next-generation HCV NS5A inhibitor discovery.

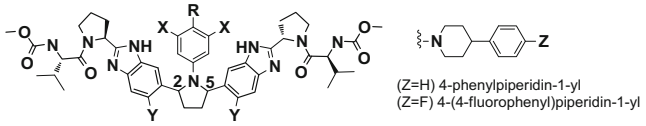

compd	pyrrolidine stereochem.	X	Y	R
27	2*S*,5*S*	H	H	t-butyl
28	2*R*,5*R*	H	H	t-butyl
29	2*R*,5*R*	H	H	F
30	2*R*,5*R*	H	H	cyclohexyl
31	2*R*,5*R*	H	H	*N*-morpholinyl
32	2*R*,5*R*	H	H	4-phenylpiperidin-1-yl
33	2*R*,5*R*	F	H	4-phenylpiperidin-1-yl
34	2*R*,5*R*	F	H	4-(4-fluorophenyl)piperidin-1-yl
35	2*R*,5*R*	H	F	t-butyl
36	2*R*,5*R*	F	F	4-phenylpiperidin-1-yl
37	2*R*,5*R*	F	F	4-(4-fluorophenyl)piperidin-1-yl

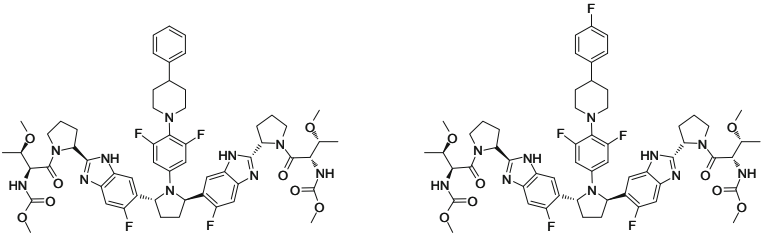

38 **PIB (Pibrentasvir, ABT-530**

Fig. 3 Structures of bis-benzimidazole NS5A inhibitors

Our first objective was to establish the structural changes required of **28**'s progeny to achieve high potencies across genotypes 1–6 and then leverage those discoveries toward compounds with significantly improved resistance profiles to maintain effectiveness against first-generation NS5A inhibitor-resistant variants. Extensive modifications of the central *N*-phenylpyrrolidine core unveiled a number of interesting observations (see Table 5). The relatively weak activity of fluorinated derivative **29** in comparison to *t*-butyl analog **28** and cyclohexyl-substituted compound **30** demonstrated the importance of substitution at the para-phenyl position. Replacement of the cyclohexyl substituent to yield the more polar morpholino derivative **31** revealed that increased hydrophilicity was not well tolerated. Although replacement of the morpholino group with the more lipophilic 4-phenyl piperidine **32** did not improve the antiviral activity across genotypes, attenuating the basicity of the piperidine ring through the introduction of fluorine at positions X and Y (**33**) did achieve that objective across genotypes 1–6. Having reached the important goal of

Table 5 Antiviral activity (EC_{50}, pM) of benzimidazole linker NS5A inhibitors in HCV stable replicons

	Inhibition of HCV stable replicons containing NS5A from genotypes 1–6 EC_{50} (pM)									
			40% H. plasma							
Compd	1a	1b	1a	1b	2a	2b	3a	4a	5a	6a
27	71	13	1,980	354	NT	NT	NT	NT	NT	NT
28	9	13	148	268	152	10	6	6	NT	NT
29	38	25	490	427	28	21	31	14	NT	14
30	4	9	107	178	10	7	8	9	NT	NT
31	379	382	902	2,070	598	960	1,200	316	NT	NT
32	324	325	1,510	1,510	468	452	481	243	NT	402
33	2	6	76	183	8	6	6	4	3	8
34	3	8	78	126	20	13	13	9	NT	21
36	2	6	58	135	8	3	4	4	2	9
37	1	3	70	172	3	2	1	1	1	3

Table 6 Pharmacokinetic parameters for selected benzimidazole-linked NS5A inhibitors[a]

		IV			Oral				
Compd	Species	$t_{1/2}$	Vss	Cl	$t_{1/2}$	T_{max}	C_{max}	AUC_{last}	F
28	Mouse[b]	2.0	0.6	0.38	2.6	1.7	0.27	1.36	11
33	Mouse	12.9	0.34	0.02	[c]NC	16	0.44	6.83	[c]NC
34	Mouse	[d]NT	[d]NT	[d]NT	[c]NC	13	0.27	4.59	[c]NC
35	Mouse	[d]NT	[d]NT	[d]NT	4.39	7.0	0.63	5.51	[c]NC
36	Mouse	[d]NT	[d]NT	[d]NT	[c]NC	15	0.99	14.0	[c]NC
37	Mouse	[d]NT	[d]NT	[d]NT	[c]NC	24	1.85	26.1	[c]NC
38	Mouse	[c]NC	0.1[e]	<0.004	[c]NC	7.0	0.96	13.8	[c]NC
	Rat	6.5	0.1[e]	0.10	6.4	3.7	0.12	1.2	5.1
	Dog	4.0	0.1[e]	0.13	3.4	4.0	0.41	4.7	24.2
	Monkey	5.4	0.1[e]	0.11	7.5	2.7	0.19	1.6	8.1
PIB	Mouse	2	0.09[e]	<0.003	[c]NC	11	1.27	20.0	[c]NC
	Rat	6.2	[d]NT	0.07	7.0	5.3	0.28	3.6	9.9
	Dog	7.1	0.1[e]	0.097	8.3	3.67	0.63	6.67	29.8
	Monkey	8.3	0.07[e]	0.15	5.69	4.0	0.29	2.25	14.1

[a]Units: $t_{1/2}$ (h); Cl (L/h/kg); C_{max} (μg/mL); $AUC_{0–24\ h}$ (μg h/mL); F (%). Routine doses: 3 mg/kg IV and oral for rat mouse, 1 mg/kg IV and 2.5 mg/kg oral for dog and monkey
[b]5 mg/kg IV and oral mouse
[c]*NC* not calculated
[d]*NT* not tested
[e]V_C (L/kg)

pan-genotype activity in replicon assays, we turned our attention to a problem that was identified with the original lead bis-benzimidazole inhibitor, **28**. Pharmacokinetic properties (Table 6) for this compound were poor across preclinical species in comparison to the bis-anilide inhibitor ombitasvir, particularly in rodent, where it

was found that very low plasma levels were obtained with oral dosing. Unexpectedly, it was found that larger and more lipophilic E-rings provided higher circulating plasma levels upon oral exposure, e.g., compounds **33** and **34**. An exploratory effort modifying the benzimidazole linker identified symmetrically substituted 5-fluorobenzimidazole analog **35** as an analog with plasma exposures that were several fold higher than that achieved with **28** upon oral administration of a similar dose in mouse [14]. Introducing the fluorine substituent into the benzimidazole groups of pan-genotype inhibitors **33** and **34** gave **36** and **37**, respectively, which provided plasma levels with oral dosing in mouse that were improved several fold in both cases. A notable feature of these compounds is the long T_{max} and significant plasma concentrations of drug at 24 h, which prevent half-life calculations but result in significant enhancement of AUC_{last}. Replicon inhibition across genotypes for **37** ranged from 1 to 3 picomolar, a potency range far better than had been achieved in any inhibitor series before, including the bis-benzimidazole series prior to fluorination of the heterocyclic groups.

Further characterization of many of these analogs also showed that progress was being made against HCV 1a and 1b NS5A first-generation inhibitor-resistant variants. Compounds were evaluated in a transient replicon assay, and fold losses in EC_{50} potencies relative to 1a and 1b NS5A "wild-type" replicons are shown in Table 7. This table illustrates the SAR of a variety of substituent patterns that, while found to show promise across wild-type genotypes 1–6, resulted in significant variation in their ability to suppress the replication of clinically relevant ombitasvir-resistant variants. Examination of the data reveals that the greatest resistance emerged with the Q30E, Y93H, and Y93N variants in genotype 1a. Y93 variants of genotype 1b, where tested, were susceptible to all analogs shown in Table 7. There appears to be a general trend that increased size at position "R" (Fig. 3) correlates with an improved ability to suppress replication with lower multiples of the wild-type EC_{50}. One particular exception to this trend is found for

Table 7 SAR of NS5A inhibitors – fold resistance of HCV genotype 1a/1b NS5A transient replicon variants vs. wild type

	HCV genotype 1a/1b NS5A variants vs. wild type (fold resistance)							
	1a[a]						1b	
Cmpd	M28T	Q30E	Q30R	Y93C	Y93H	Y93N	Y93H	Y93N
28	4	61	14	7	216	510	2	NT
30	>17	>90	>20	>30	>577	NT	1	NT
31	2	6	7	5	87	NT	1	NT
32	2	4	3	2	4	5	1	1
33	3	69	7	6	72	145	1	1
34	2	20	3	3	20	25	2	NT
36	1	12	2	6	49	50	1	1
38	1	2	1	1	6	5	1	0.3
PIB	2.1	2.4	1.7	1.7	6.7	6.7	0.6	0.6

[a]Observed as resistant variants in ombitasvir single-agent clinical studies

30, where the wild-type EC_{50} was more potent than the lowest concentration tested. Although the fold resistance pattern for **32** is superior to any other compound in Table 7, it should be noted that Table 5 shows the pan-genotype replicon potencies for this compound to be much weaker than **33**, **34**, and **36**. Indeed these three compounds come close to fulfilling the virology profile requirements for a next-generation analog and deliver a profound improvement in performance against resistant variants when compared to the first-generation NS5A inhibitor ombitasvir or **28**, while demonstrating good PK in mouse (Table 6).

The beneficial effects observed by introduction of fluorine atoms at several key positions in our developing chemical matter were sufficiently noteworthy to the team so that we favored late-stage research activities to include these structural modifications. As the majority of the early and intermediate medicinal chemistry activities focused on the central and linker regions of the lead structures in both the first-generation and next-generation efforts, it was observed that substitution of the Moc-Val capping groups also affected the virological properties. In particular, efforts in the first-generation medicinal chemistry studies showed that oxygen-containing amino acids could beneficially affect the resistance profile of the resulting analogs (data not shown). The intriguing possibility of importing those observations into the next-generation medicinal chemistry effort resulted in the synthesis of the Moc-methyl-threonine-capped compounds shown in Table 8. Analogs **38** and PIB (pibrentasvir, ABT-530) demonstrated potent inhibition of the HCV replicon across genotypes 1–6. However, just as gratifying were the very low fold losses measured against the first-generation NS5A inhibitor-resistant variants, thus achieving two critical project objectives (Table 7) [15]. Upon oral administration in mouse, the plasma exposures of both compounds compare favorably to prior compounds in Table 6. Interestingly, both compounds show much lower exposures in rat than in mouse, with plasma exposure in dog showing better performance than either monkey or rat. While the virology of both compounds are similar, PIB's PK properties do seem to show a slight advantage, and it was therefore elevated to clinical status.

Pibrentasvir was further characterized to determine how frequently resistant colonies would emerge from replicons containing NS5A genes from genotypes 1a, 1b, 2a, 2b, 3a, 4a, 5a, and 6a at both 10× and 100× of the WT EC_{50}s (Table 9) [15]. After determining the resistant NS5A gene sequences that conferred resistance, mean EC_{50}s of PIB against these variants (and therefore fold resistance vs. WT in transient replicons containing these single or double point mutations) were measured, as well as replication efficiency to estimate the mutant's "fitness." No surviving colonies were detected when HCV 1b, 2b, 4a, 5a, and 6a NS5A-containing replicons were incubated in the presence of 10× or 100× of PIB's EC_{50}. Upon incubation with PIB at 10× EC_{50}, genotypes 1a, 2a, and 3a showed colony survival of 0.0065%, 0.00015%, and 0.0003%, respectively. At 100× EC_{50}, only genotype 1a NS5A containing replicons survived the incubation with a frequency of 0.0002%. At 10× EC_{50}, replicons of genotype 1a and 3a display the Y93H resistant variant as either the most frequently prevalent or only surviving colony detected, and genotype 2a displays only two colonies both of which possess amino acid changes at two locations (F28S/M21I or P29S/K30G). At 100× EC_{50}, only genotype 1a NS5A

Table 8 Antiviral activity (EC_{50}, pM) of Moc-*O*-methyl-Thr-capped NS5A inhibitors in HCV stable replicons

	Inhibition of HCV stable replicons containing NS5A from genotypes 1–6 EC_{50} (pM)									
			40% H. plasma							
Compd	1a	1b	1a	1b	2a	2b	3a	4a	5a	6a
38	1	3	43	138	3	3	3	3	2	4
PIB	1.8 ± 0.86	4.3 ± 1.7	64 ± 14	200 ± 54	2.3 ± 0.65	1.9 ± 0.59	2.1 ± 0.66	1.9 ± 0.61	1.4 ± 0.36	2.8 ± 0.67

Table 9 Selection of NS5A amino acid substitutions by PIB in replicon cell lines with NS5A from HCV genotypes 1–6 and resistance of these substitutions to pibrentasvir

Genotype[a]	Colony survival (%)[b]		NS5A amino acid substitutions	Prevalence in replicon selection[c]		Mean EC_{50} ± SD (pM)	Fold change in EC_{50}[d]	Replication efficiency[d] (%)
	10× EC_{50}	100× EC_{50}		10× EC_{50}	100× EC_{50}			
1a[e]	0.0065	0.0002	Q30D[f]	0/20	1/4[g]	68 ± 37	94	50
			Q30 deletion	0/20	1/4[g]	2,555 ± 268	3,549	0.5
			Y93D	0/20	1/4[g]	NV	NV	<0.5
			Y93H	18/20	0/4[g]	4.8 ± 1.5	6.7	18
			Y93N	1/20	0/4[g]	5.1 ± 2.1	7.1	25
			H58D + Y93H	0/20	1/4[g]	1,612 ± 272	2,238	13
1b	0	ND	NA	NA	NA	NA	NA	–
2a[e]	0.00015	0	F28S + M31I	2/3 g	NA	14,303 ± 2,722	14,448	–
			P29S + K30G	1/3 g	NA	2.3 ± 0.36	2.3	–
2b	0	0	NA	NA	NA	NA	NA	–
3a[e]	0.0003	0	Y93H	3/3[h]	NA	1.5 ± 0.19	2.3	–
4a	0	0	NA	NA	NA	NA	NA	–
5a	0	0	NA	NA	NA	NA	NA	–
6a	0	0	NA	NA	NA	NA	NA	–

NA not applicable, *ND* not done, *NV* not available, as the EC_{50} value could not be determined due to low replication efficiency of the replicon containing the amino acid substitution

[a]Genotype of NS5A in replicon cell lines

[b](Number of surviving colonies/number of input replicon cells) × 100

[c]Number of times an amino acid substitution was found out of the total number of colonies analyzed

[d]Relative to the respective wild-type replicon

[e]EC_{50} values for wild-type replicons in transient transfection assays: genotype 1a = 0.72 pM, genotype 2a = 0.99 pM, and genotype 3a = 0.65 pM

[f]Substitution with double nucleotide changes

[g]Denominator indicates total number of colonies that survived selection out of 2×10^6 input cells

[h]Denominator indicates total number of colonies that survived selection out of 1×10^6 input cells

replicons show survival, with only four colonies detected starting from 2×10^6 input cells. The genotype 1a NS5A mutants with the highest fold resistance are the Q30 deletion and H58D + Y93H variants with a fold change in EC_{50} of 3,549-fold and 2,238-fold vs. WT, respectively. However, the replication efficiency of replicons containing these changes is significantly lower at 0.5% and 13% of WT. The Q30D mutation shows the highest replication efficiency at 50%, conferring a 94-fold change in EC_{50} relative to WT.

4 Clinical Studies

PIB in combination with glecaprevir (GLE, ABT-493) has been the subject of multiple clinical studies, having successfully completed phase I–III studies in the USA and abroad. The combination GLE/PIB (trade name Mavyret in the USA and Maviret in Europe) was approved in the USA and Europe in August 2017. A partial summary of some of these clinical studies is shown below.

SURVEYOR-1 (genotypes 1, 4, 5, and 6) and SURVEYOR-2 (genotypes 2 and 3) were phase II, open-label, multicenter dose-ranging trials in non-cirrhotic patients with chronic HCV genotype 1–6 infection who were either previously untreated or only treated with pegylated interferon plus ribavirin (Table 10) [16]. Doses of GLE and PIB were varied, with or without ribavirin (RBV, total daily dose 1,000 mg for patients $<$75 kg or 1,200 mg for patients $\geq$75 kg) for 8 or 12 weeks. Primary efficacy endpoints were the percentage of patients that achieved a sustained virologic response 12 weeks after completing treatment (SVR12).

Across all studies 319/449 (70%) patients experienced adverse events, with the majority reported as mild in severity. The most common ($\geq$10%) adverse events in RBV-free treatment were fatigue, headache, and nausea, with a greater frequency of these events occurring in RBV-treated patients. Three patients discontinued treatment prematurely due to adverse events. Serious adverse events were reported in seven patients, none of which were considered to be related to the study drugs. Table 10 shows that the most difficult to treat patients were infected with genotype 3, with the higher dose combination of 300 mg GLE and 120 mg PIB demonstrating superior efficacy than the lower dose combinations. Based on this observation, combined with the desire to maintain a consistent dosing paradigm across patients in genotypes 1–6, this particular dose combination was chosen for further studies. For treatment-naïve or PEG-IFN/RBV-treated HCV genotype 1, 2, 4–6 patients, SVR12 was achieved at between 96 and 100% of the patient groups tested, with no significant differences detected between 8- and 12-week treatment durations in genotype 2 patients. In genotype 3, for the treatment arm containing both treatment-naïve and PEG-IFN/RBV-treated individuals, 12 weeks of treatment at 300 mg GLE and 120 mg PIB resulted in 28/30 (93%) patients achieving SVR. Two separate treatment arms receiving the same doses had the treatment-naïve patients achieving 28/29 (97%) SVR_{12} after 8 weeks of treatment and the PEG-IFN/RBV-treated individuals achieving 22/24 (92%) SVR_{12} after 12 weeks of treatment.

Table 10 SURVEYOR-1 and SURVEYOR-2 virologic response during and after treatment and reasons for non-response

Genotype	Prior Tx history	Dose GLE + PIB	Tx duration (weeks)	Sustained virologic response, n/N (%)		Reasons for non-response, n (%)			
						Virologic failure		Non-virologic failure	
				PTW4	PTW12[a]	Breakthrough	Relapse	Missing SVR12 data	Early Tx discontinuation
1	TN or PR	200 + 120	12	40/40 (100)	40/40 (100)	0	0	0	0
	TN or PR	200 + 40	12	38/39 (97)	38/39 (97)	0	1 (3)	0	0
	TN or PR	300 + 120	8	34/34 (100)	33/34 (97)	0	0	0	1 (3)
2	TN or PR	300 + 120	12	24/25 (96)	24/25 (96)	0	0	0	1 (4)
	TN or PR	200 + 120	12	24/24 (100)	24/24 (100)	0	0	0	0
	TN or PR	200 + 120 + RBV[b]	12	25/25 (100)	25/25 (100)	0	0	0	0
	TN or PR	300 + 120	8	53/54 (98)	53/54 (98)	0	0	0	1 (2)
3	TN or PR	300 + 120	12	28/30 (93)	28/30 (93)	0	1 (3)	1 (3)	0
	TN or PR	200 + 120	12	28/30 (93)	28/30 (93)	0	2 (7)	0	0
	TN or PR	200 + 120 + RBV[b]	12	29/31 (94)	29/31 (94)	1 (3)	0	0	1 (3)[c]
	TN or PR	200 + 40	12	28/30 (93)	25/30 (83)	1 (3)	2 (7)	1 (3)	1 (3)
	TN	300 + 120	8	28/29 (97)	28/29 (97)	0	0	1 (3)	0
	PR	300 + 120	12	23/24 (96)	22/24 (92)	1 (4)	1 (4)	0	0
4, 5, 6	TN or PR	300 + 120[d]	12	34/34 (100)	34/34 (100)	0	0	0	0

Tx treatment, *PTW* post treatment week, SVR_{12} sustained virologic response at post treatment week 12, *TN* treatment naïve, *PR* peg-IFN/RBV-experienced, *RBV* ribavirin

[a]Primary endpoint

[b]RBV total daily dose 1,000 mg for patients <75 kg or 1,200 mg for patients ≥75 kg

[c]Patient discontinued treatment at week 10 and was found to be reinfected with HCV genotype 1a during post treatment follow-up

[d]Includes two patients who received GLE 200 mg + PIB 120 mg for 12 weeks

On- or post treatment virologic failure occurred in 10/449 (2%) of the treated patients. One genotype 1a patient who received the lowest GLE/PIB dose combination experienced relapse post treatment at week 4. The remaining nine patients with virologic failure were infected with genotype 3a with 6/9 receiving doses lower than the most effective GLE/PIB combination which was discovered during this dose-ranging study.

ENDURANCE-1 and ENDURANCE-3 were two phase III randomized, open-label, multicenter trials treating a total of 1,208 non-cirrhotic patients infected with either HCV genotype 1a/b or 3, which compared the outcomes of treating patients with 300 mg GLE and 120 mg PIB QD for either 8 or 12 weeks (Table 11) [17]. In the genotype 3 patient cohort, 1/3 of the patients enrolled were dosed with sofosbuvir-daclatasvir for 12 weeks in order to compare this patient outcome to the 8- and 12-week GLE/PIB HCV genotype 3 patient arms. Non-cirrhotic patients who presented positive for HCV genotype 1 infection could also be coinfected with HIV-1 and could either not have received treatment for HCV or have received an IFN-containing regimen with or without ribavirin or treatment with sofosbuvir with or without PEG-IFN. Genotype 3 patients needed to be treatment naïve. The safety profile of GLE/PIB in all patients was similar with the most common adverse effects ($\geq$10%) being headache and fatigue. Serious adverse events were reported in 1–2% of treated patients with none deemed to be related to the trial drugs. The results of these trials are summarized in Table 11. The results show that a high rate of HCV genotype 1- and 3-infected patients achieved SVR12 in both 8- and 12-week treatment times.

At baseline, the characteristics of patients were generally similar, but there were some notable differences. Among genotype 3-infected patients, prevalence of stage F3 fibrosis was higher in the 8-week GLE/PIB group (17%, as compared with 8–9%). The baseline HCV RNA levels in genotype 3 patients were 6 million IU/mL or higher in the 12-week GLE/PIB arm than in the SOF/DAC arm (28% vs. 12%). In this study, genotype 1 patients experienced the highest level of SVR12 upon treatment with GLE/PIB with the 8-week arm statistically demonstrating non-inferiority to the 12-week arm (348/351 patients and 351/352 patients, respectively). Genotype 3 patients treated for 12 weeks with GLE/PIB achieved SVR12 at a slightly lower rate in 222 out of 233 patients, whereas the 8-week arm achieved SVR12 rate of 149 out of 157 patients. Statistical analysis of these genotype 3 results showed non-inferiority of the 8-week regimen when compared to the 12-week treatment. Interestingly, the genotype 3 patients receiving 12 weeks of SOF/DAC achieved an SVR12 in 111 out of 115 patients. A statistical comparison showing superiority of 12 weeks of treatment of GLE/PIB was not attempted because of a statistical procedure which required both non-inferiority criteria to be met for the comparison between the 8-week and 12-week GLE/PIB treatment arms in order to proceed to testing the next ordered comparison.

As a result of these and other studies, the USA FDA approved Mavyret in August 2017 for the treatment of chronic hepatitis C viral infections of genotypes 1–6. Treatment duration is dependent on prior patient treatment experience, genotype, and whether or not the individual is non-cirrhotic or presents with compensated

Table 11 ENDURANCE-1 and ENDURANCE-3 treatment outcomes in the intention-to-treat population

Genotype	Tx	Tx duration (weeks)	Number of patients	SVR12	Reasons for failure, n (%)					
					Virologic failure		Non-virologic failure			
					Break-through	Relapse	Follow-up loss or missing SVR12 data	Early Tx discontinuation	Consent withdrawn	Nonadherence
1	GLE/PIB	12	352	351 (99.7)	0	0	1 (<1)	0	0	0
1	GLE/PIB	8	351	348 (99.1)	1 (<1)	0	1 (<1)	1 (<1)	0	0
3	GLE/PIB	12	233	222 (95)	1 (<1)	3 (1)[a]	4 (2)	1 (<1)	1 (<1)	1 (<1)
3	GLE/PIB	8	157	149 (95)	1 (1)	5 (3)	2 (1)	0	0	0
3	SOF/DAC	12	115	111 (97)	0	1 (1)	2 (2)	1 (1)	0	0

Tx treatment, *SVR12* sustained virologic response at post treatment week 12, *GLE/PIB* 300 mg glecaprevir/120 mg pibrentasvir QD, *SOF/DAC* 400 mg sofosbuvir/60 mg daclatasvir QD

[a]One patient had reinfection with HCV genotype 3, as determined by phylogenetic analysis

cirrhosis (Child-Pugh A). The shortest treatment period is 8 weeks for non-cirrhotic treatment-naïve individuals with HCV genotypes 1–6. Treatment of patients with no prior HCV treatment that present with compensated cirrhosis (Child-Pugh A) requires 12 weeks of therapy. Those that have received prior treatment are categorized according to genotype, treatment type, and cirrhotic state (no cirrhosis or compensated cirrhosis (Child-PughA)). Depending on category, treatment can be as short as 8 weeks or as long as 16 weeks.

From first-generation NS5A inhibitors, such as daclatasvir, ledipasvir, elbasvir, and ombitasvir, to the next-generation inhibitors such as velpatasvir and pibrentasvir, all have had a profound and powerful impact on the IFN-sparing treatment of HCV infection. These inhibitors, in combination with orthogonally mechanistic inhibitors, have allowed regimens that are better tolerated than IFN-based treatment and which have therefore unsurprisingly encouraged higher patient compliance. In combination, all this has resulted in higher cure rates, shorter treatment periods, improved convenience, fewer side effects, and ultimately lower costs for a cure. Moreover, it is expected that curing hepatitis C will not only reduce the burden on the healthcare system by reducing the rates of cirrhosis and hepatic carcinoma, but reduce the additional emotional and economic costs that HCV morbidity brings to patients' lives and their families.

Compliance with Ethical Standards

Funding All research described was funded by AbbVie.

Conflict of Interest All authors are employees of AbbVie and may own stock in the same.

Ethical Approval All applicable international, national, and/or institutional guidelines for the care and use of animals were followed.

All procedures performed in studies involving human participants were in accordance with the ethical standards of the institutional and/or national research committee and with the 1964 Helsinki declaration and its later amendments or comparable ethical standards.

Informed Consent Informed consent was obtained from all individual participants included in the clinical studies.

References

1. Liu Y, Lim BH, Jiang WW, Flentge CA, Hutchinson DK, Madigan DL, Randolph JT, Wagner R, Maring CJ, Kati WM, Molla A (2012) Identification of aryl dihydrouracil derivatives as palm initiation site inhibitors of HCV NS5B polymerase. Bioorg Med Chem Lett 22: 3747–3750
2. Kati W, Koev G, Irvin M, Beyer J, Liu Y, Krishnan P, Reisch T, Mondal R, Wagner R, Molla A, Maring C, Collins C (2015) In vitro activity and resistance profile of dasabuvir, a non-nucleoside HCV polymerase inhibitor. Antimicrob Agents Chemother 59:1505–1511
3. Tellinghuisen TL, Marcotrigiano J, Rice CM (2005) Structure of the zinc-binding domain of an essential component of the hepatitis C virus replicase. Nature 435:374–379
4. Kempf DJ, Norbeck DW, Codacovi L, Wang XC, Kohlbrenner WE, Wideburg NE, Paul DA, Knigge MF, Vasavanonda S, Craig-Kennard A, Saldivar A, Rosenbrook Jr W, Clement JJ,

Plattner JJ, Erickson J (1990) Structure-based C-2 symmetric inhibitors of HIV protease. J Med Chem 33:2687–2689
5. Bachand C, Belema M, Deon DH, Good AC, Goodrich J, James CA, Lavoie R, Lopez OD, Martel A, Meanwell NA, Nguyen VN, Romine JL, Ruediger E, Snyder LB, St. Laurent DR, Yang F, Langley DR, Wang G, Hamann LG Hepatitis C virus inhibitors. WO 2008/021927 World International Property Organization
6. DeGoey DA, Betebenner DA, Grampovnik DJ, Liu D, Pratt JK, Tufano MD, He W, Krishnan P, Pilot-Matias TJ, Marsh KC, Molla A, Kempf DJ, Maring CJ (2013) Discovery of pyrido[2,3-d] pyrimidine-based inhibitors of HCV NS5A. Bioorg Med Chem Lett 23:3627–3630
7. Zheng GZ, Lee CH, Pratt JK, Perner RJ, Jiang MQ, Gomtsyan A, Matulenko MA, Mao Y, Koenig JR, Kim KH, Muchmore S, Yu H, Kohlhaas K, Alexander KM, McGaraughty S, Chu KL, Wismer CT, Mikusa J, Jarvis MF, Marsh K, Kowaluk EA, Bhagwat SS, Stewart AO (2001) Pyridopyrimidine analogues as novel adenosine kinase inhibitors. Bioorg Med Chem Lett 11: 2071–2074
8. Krishnan P, Beyer J, Mistry N, Koev G, Reisch T, De Goey D, Kati W, Campbell A, Williams L, Xie W, Setze C, Molla A, Collins C, Pilot-Matias T (2015) *In vitro* and *in vivo* antiviral activity and resistance profile of ombitasvir, an inhibitor of hepatitis C virus NS5A. Antimicrob Agents Chemother 59(2):979–987
9. DeGoey DA, Randolph JT, Liu D, Pratt J, Hutchins C, Donner P, Krueger AC, Matulenko M, Patel S, Motter CE, Nelson L, Keddy R, Tufano M, Caspi DD, Krishnan P, Mistry N, Koev G, Reisch TJ, Mondal R, Pilot-Matias T, Gao Y, Beno DWA, Maring CJ, Molla A, Dumas E, Campbell A, Williams L, Collins C, Wagner R, Kati WM (2014) Discovery of ABT-267, a pan-genotypic inhibitor of HCV NS5A. J Med Chem 57:2047–2057
10. Lawitz E, Marbury T, Campbell A, Dumas E, Kapoor M, Pilot-Matias T, Krishnan P, Setze C, Xie W, Podsadecki T, Bernstein B, Williams L (2012) Safety and antiviral activity of ABT-267, a novel NS5A inhibitor, during 3-day monotherapy: first study in HCV genotype-1 (gt1)-infected treatment-naive subjects. J Hepatol 56:S469–S470
11. Badri PS, Shuster DL, Dutta S, Menon RM (2017) Clinical pharmacokinetics of ombitasvir. Clin Pharmacokinet 56:1103–1113
12. Dumas E, Lawal A, Menon RM, Podsadecki T, Awni W, Dutta S, Williams L (2011) Pharmacokinetics, safety and tolerability of the HCV NS5A inhibitor ABT-267 following single and multiple doses in healthy adult volunteers. J Hepatol 54(Suppl 1):S475–S476
13. Wagner R, Randolph JT, Patel SV, Nelson L, Matulenko MA, Keddy R, Pratt JK, Liu D, Krueger AC, Donner PL, Hutchinson DK, Flentge C, Betebenner D, Rockway T, Maring CJ, Ng TI, Krishnan P, Pilot-Matias T, Collins C, Panchal N, Reisch T, Dekhtyar T, Mondal R, Stolarik DF, Gao Y, Gao W, Beno DA, Kati WM (2018) Highlights of the structure activity relationships of benzimidazole linked pyrrolidines leading to the discovery of the HCV NS5A inhibitor pibrentasvir (ABT-530). J Med Chem 61(9):4052–4066
14. Randolph JT, Flentge CA, Donner P, Rockway TW, Patel SV, Nelson L, Hutchinson DK, Mondal R, Mistry N, Reisch T, Dekhtyar T, Krishnan P, Pilot-Matias T, Stolarik DF, Beno DWA, Wagner R, Maring C, Kati WM (2016) Discovery of fluorobenzimidazole HCV NS5A inhibitors. Bioorg Med Chem Lett 26:5462–5467
15. Ng TI, Krishnan P, Pilot-Matias T, Kati W, Schnell G, Beyer J, Reisch T, Lu L, Dekhtyar T, Irvin M, Tripathi R, Maring C, Randolph JT, Wagner R, Collins C (2015) In vitro antiviral activity and resistance profile of the next-generation hepatitis C virus NS5A inhibitor pibrentasvir. Antimicrob Agents Chemother 61(5):e02558-16/1–e02558-16/14
16. Kwo PY, Poordad F, Asatryan A, Wang S, Lin C-W, Liu R, Lovell SS, Ng TI, Kort J, Mensa FJ, Wyles DL, Hassanein T, Felizarta F, Sulkowski MS, Gane E, Maliakkal B, Overcash JS, Gordon SC, Muir AJ, Aguilar H, Agawal K, Dore GJ (2017) Glecaprevir and pibrentasvir yield high response rates in patients with HCV genotype 1-6 without cirrhosis. J Hepatol 67(2):263–271
17. Zeuzem S, Foster GR, Wang S, Asatryan A, Gane E, Feld JJ, Asselah T, Bourliere M, Ruane PJ, Wedemeyer H, Pol S, Flisiak R, Poordad F, Chuang W-L, Stedman CA, Flamm S, Kwo P, Dore GJ, Sepulveda-Arzola G, Roberts SK, Soto-Malave R, Kaita K, Puoti M, Vierling J, Tam E, Vargas HE, Bruck R, Fuster F, Paik S-W, Felizarta F, Kort J, Fu B, Liu R, Ng TI, Pilot-Matias T, Lin C-W, Trinh R, Mensa FJ (2018) Glecaprevir-pibrentasvir for 8 or 12 weeks in HCV genotype 1 or 3 infection. N Engl J Med 378:354–369